PNAS
www.pnas.org

Main Manuscript for

Hydrogen sulfide is neuroprotective in Alzheimer's disease by sulfhydrating GSK3β and inhibiting Tau hyperphosphorylation.

Daniel Giovinazzo[1], Biljana Bursac[5], Juan I Sbodio[1], Sumedha Nalluru[1], Thibaut Vignane[5], Adele M. Snowman[1], Lauren M. Albacarys[1], Thomas W. Sedlak[2], Roberta Torregrossa[4], Matthew Whiteman[4], Milos R. Filipovic[5], Solomon H. Snyder[1,2,3]* and Bindu D. Paul[1]*

[1]The Solomon H. Snyder Department of Neuroscience, [2] Department of Psychiatry and Behavioral Sciences, [3]Department of Pharmacology and Molecular Sciences, Johns Hopkins University School of Medicine, Baltimore, MD 21205, United States. [4]Medical School Building, University of Exeter, Exeter, United Kingdom. [5]Leibniz-Institut für Analytische Wissenschaften - ISAS - e.V., Dortmund, Germany.

Correspondence to:

* Bindu D. Paul; Solomon H. Snyder

Email: bpaul8@jhmi.edu

ssnyder@jhmi.edu

Classification: Biology, Neuroscience

Keywords

Alzheimer's disease, Hydrogen sulfide, Tau, Sulfhydration, Persulfidation, Cystathionine γ-lyase, NaGYY

Author Contributions

BDP conceptualized the study. BDP, DG and SHS designed the study. DG, BDP, BB, JIS, SN, TV, AMS and MRF conducted experiments. MW and RT provided synthesized ultra-pure H_2S donors and helped design animal dosage. TWS provided tools/reagents. LMA helped with animal care, genotyping and maintenance. DG, MRF, SHS and BDP analyzed data. DG, SHS and BDP wrote the paper with input from all the authors.

This PDF file includes:

Main Text, Figures 1 to 4

Abstract

Alzheimer's disease (AD), the most common cause of dementia and neurodegeneration in the elderly, is characterized by deterioration of memory, executive and motor functions. Neuropathologic hallmarks of AD include neurofibrillary tangles, paired helical filaments and amyloid plaques. Mutations in the microtubule associated protein, Tau, a major component of the neurofibrillary tangles, cause its hyperphosphorylation in AD. We have shown that signaling by the gaseous signaling molecule, hydrogen sulfide (H_2S), is dysregulated during aging. H_2S signals via a posttranslational modification termed sulfhydration/persulfidation, which participates in diverse cellular processes. Here we show that cystathionine γ-lyase (CSE), the biosynthetic enzyme for H_2S, binds wild type Tau, which enhances its catalytic activity. By contrast, CSE fails to bind Tau P301L, a mutant that is hyperphosphorylated in the 3xTg-AD mouse model of AD. We further show that CSE is depleted in 3xTg-AD mice as well as in human AD brains, H_2S prevents phosphorylation of Tau by sulfhydrating its kinase, glycogen synthase kinase 3β (GSK3β). Finally, we demonstrate that sulfhydration is diminished in AD, while administering the H_2S donor, sodium GYY4137 (NaGYY), to the 3xTg-AD mice ameliorates motor and cognitive deficits in AD.

Significance Statement

Alzheimer's disease (AD) is the leading cause of dementia in the elderly. Although dysregulated hydrogen sulfide (H_2S) metabolism has been reported in AD, and H_2S donors are beneficial, molecular mechanisms underlying neuroprotective effects of H_2S are largely unknown. We now show that H_2S confers neuroprotection by sulfhydrating GSK3β, to inhibit its activity, thereby preventing hyper-phosphorylation of Tau, a key pathogenic event in AD. Administering H_2S donors improves motor and cognitive functions in a mouse model of AD.

Introduction

Alzheimer's disease (AD), the most prevalent neurodegenerative disorder, involves loss of memory and executive functions (1, 2). Currently no cure exists for AD, and clinical trials of diverse agents have largely failed to demonstrate therapeutic benefit (3, 4). AD may occur sporadically or have a genetic origin, with several mutations linked to a high risk for the disease (5). AD is characterized by aggregation of the microtubule associated protein, Tau and β-amyloid peptides, which are components of neurofibrillary tangles (NFTs) and amyloid plaques respectively (2, 3, 6). AD belongs to the class of diseases termed tauopathies, which include progressive supranuclear palsy (PSP), corticobasal degeneration (CBD), Pick's disease and frontotemporal lobar degenerative

disorders (FTLD) (7, 8). Tau was originally identified as a microtubule binding protein, which mediates assembly of microtubules (9). Tau undergoes several post-translational modifications *in vivo*, including phosphorylation, sumoylation and acetylation (10-13). Disease progression in AD is closely linked to Tau pathology (14, 15). Hyperphosphorylation of Tau, a hallmark of AD, decreases its binding to microtubules and causes its aggregation and mislocalization leading to neurotoxicity via multiple mechanisms, including changes in cytoskeletal architecture, axonal transport and mitochondrial respiration. (16-20).

AD is associated with increased oxidative stress which promotes neurodegeneration (21). The reverse transsulfuration pathway leading to the synthesis of cysteine and glutathione (GSH) helps maintain redox homeostasis in the brain (Fig. 1*A*) and is dysregulated in neurotoxicity and neurodegeneration (22-26). Cystathionine γ-lyase (CSE) is the biosynthetic enzyme for the gaseous signaling molecule hydrogen sulfide (H_2S) as well as its precursor cysteine (27)(Fig. 1*A*). CSE utilizes cystathionine which is synthesized from homocysteine by cystathionine β-synthase (CBS), to generate cysteine (28). Both CSE and CBS synthesize H_2S in the brain, with CSE expressed in neurons and CBS in astrocytes (29). H_2S is formed endogenously in almost all tissues and signals by sulfhydration/persulfidation (27, 30-33). Like nitric oxide (NO) and carbon monoxide (CO), H_2S is a gasotransmitter with pleiotropic roles (27, 34). Apart from its role as an endothelial derived relaxation factor (EDRF), H_2S has neuroprotective functions at physiological concentrations (34-37). We have shown previously that disrupted metabolism of cysteine and H_2S may be pathogenic in neurodegenerative conditions such as Parkinson's disease (PD) and Huntington's disease (HD) (24, 25, 38). Sulfhydration is an evolutionarily conserved process, which is diminished during aging (39). Depletion of cysteine, a product of the reverse transsulfuration pathway, is also associated with aging and neurodegeneration (40, 41). We now report that the reverse transsulfuration pathway and persulfidation are dysregulated in AD while supplementation with H_2S donors is beneficial. Moreover. motor and cognitive deficits are mitigated by administration of H_2S donors.

Results

Dysregulation of the reverse transsulfuration pathway in AD

Previously we reported altered H_2S metabolism and sulfhydration patterns in PD, while administering H_2S donors proved beneficial in mouse models of PD (9, 10). Similarly, in mouse models of AD, H_2S donors reversed disease symptoms and improved spatial and cognitive deficits (42, 43). We analyzed the expression of CSE in AD mouse models as well as human post-mortem samples. We utilized the 3xTg-AD mouse model of AD, which harbors the mutations PS1M146V, APPSwe and Tau P301L and develops both neurofibrillary tangles and amyloid plaques (44). CSE expression was reduced in the cerebral cortex and hippocampus of these mice (Fig. 1*B,C*).

Moreover, we observed a 50% decrease in CSE expression in the cortex of AD postmortem brain (Fig. 1*D*). Using the dimedone-switch assay, we observed decreased levels of overall sulfhydration (Fig. 1*E,F*).

CSE and CBS interact with wild type but not Tau P301L

As H_2S levels and sulfhydration are decreased in AD patients, we explored the interaction of CSE and CBS, the major H_2S producing enzymes, with Tau and amyloid precursor protein (APP), proteins, which constitute the NFTs and amyloid plaques respectively. Neither CSE nor CBS bound APP (*SI Appendix*, Fig. S1A, B). In the adult brain Tau exists as six isoforms derived by alternative splicing (45) . We utilized full length Tau comprising 441 amino acid residues, which is also present in neurons (46)(Fig. 2*A*). CSE and CBS bind to wild type Tau in HEK293 cells overexpressing CSE or CBS and Tau (Fig. 2*B*). Next, we studied the interaction of Tau and CSE, purified from bacterial cells (*SI Appendix,* Fig. S2). Purified CSE and Tau also interacted, indicating that CSE binds Tau directly (Fig. 2*C*). As the 3xTg-AD mouse model harbors the mutant, Tau P301L, we studied the binding of CSE and CBS to this mutant in HEK293 cells. Both CSE and CBS did not bind the P301L mutant of Tau (Fig. 2*D*). In the case of CBS, using GFP-Tau, we observed additional bands migrating above the band corresponding to GFP-Tau, likely reflecting non-specific bands (Fig. 2*D*). In the case of Flag-Tau, additional bands were not observed (Fig. 2*B*). As Tau is a neuronal protein and CSE, but not CBS, resides in neurons, with CBS being localized to astrocytes, we focused the remainder of our studies on CSE. We analyzed the influence of Tau on CSE activity by measuring H_2S production from L-cysteine in the presence of its cofactor, pyridoxal 5-phosphate (PLP). Purified tau enhanced H_2S production from human recombinant CSE *in vitro* (Fig. 2*E,F*). We also measured H_2S production (by supplementing with L-cysteine and PLP) from the lysates of HEK293 cells transfected with CSE and Tau (Fig. 2*G*). CSE activity increased with time, and wild type Tau further augmented H_2S generation by CSE (Fig. 2*H*). As CSE is the biosynthetic enzyme for H_2S in neurons and signals by sulfhydration, we assessed whether Tau is sulfhydrated by CSE. Tau contains two cysteine residues, Cys291 and Cys322, which could be sulfhydrated (Fig. 2*A*). We monitored Tau sulfhydration in transfected HEK293 cells using the modified biotin switch assay (Fig. 2*I*), as well as the dimedone switch method in conjunction with mass spectrometry, which revealed that Tau is indeed sulfhydrated at C322 (*SI Appendix*, Fig. S5).

H_2S generated by CSE inhibits phosphorylation of Tau by glycogen synthase kinase β

Tau harbors several sites which are phosphorylated by multiple kinases. Hyperphosphorylation of Tau decreases its affinity for microtubules and causes its aggregation. One of the major kinases which phosphorylates Tau is glycogen synthase kinase β (GSK3β), a serine/threonine kinase, which modifies several sites on the protein *in vivo* (47). We wondered whether CSE and H_2S

modulate Tau phosphorylation by GSK3β. To explore the effect of H_2S on Tau phosphorylation, we utilized purified Tau, CSE and GSK3β in an *in vitro* assay (Fig. 3*A*). Phosphorylation of Tau at Ser396 by GSK3β was significantly diminished when CSE in combination with L-cysteine and PLP, the substrate and cofactor for CSE respectively, were added to the reaction mixture (containing CSE, Tau and ATP as described in the Materials and Methods), indicating a role for H_2S. Consistent with this observation, phosphorylation of Tau was reduced when sodium hydrosulfide (NaSH) was added alone to GSK3β, Tau and ATP, in the absence of CSE, L-cysteine and PLP (Fig. 3*A*). To determine whether the cysteines in Tau affect its phosphorylation, we mutated these residues to serine and conducted the phosphorylation assays with GSK3β. Phosphorylation of the mutant, Tau C291S/C322S, was inhibited as well, indicating that absence of cysteine residues does not prevent the inhibition of Tau phosphorylation by GSK3β (Fig. 3*B*). As GSK3β is inhibited by phosphorylation of its Ser9 residue by the endogenous kinase, Akt, we explored whether the inhibitory effect of H_2S on phosphorylation of Tau involves Ser9 of GSK3β. We utilized a constitutively active mutant of GSK3β, GSK3β S9A, wherein Ser9 is mutated to Ala (and therefore is not subject to inhibition by Akt) and examined the effect of H_2S on phosphorylation of Tau. We analyzed Tau phosphorylation in HEK293 cells using the mutant, Tau P301L, which is a mutation present in the 3xTg-AD mouse model of AD (44). NaSH inhibited phosphorylation of Tau P301L even when GSK3β S9A was present, indicating that H_2S acts by a mechanism independent of phosphorylation of GSK3β at Ser9 (Fig. 3*C*). Similarly, H_2S also inhibited phosphorylation of the C291S/C322S mutant of Tau P301L in HEK293 cells, further confirming that inhibition of Tau phosphorylation does not require the cysteine residues on Tau (Fig. 3*C*). In HEK293 cells, phosphorylation of Tau resulted in its slower migration on gels, as reported previously (48). Treatment with NaSH inhibited phosphorylation at Ser396 and resulted in faster mobility of Tau P301L on the gel (Fig. 3*C*). NaSH also inhibited phosphorylation of Tau at Ser202 and Thr205 (*SI Appendix*, Fig. S3A). Moreover, total Tau levels were increased in the GSK3β transfected samples, which may reflect stabilization of Tau P301L by GSK3β, which could result in increased accumulation of Tau and neurotoxicity. To further characterize inhibition of GSK3β activity by H_2S, we conducted activity assays using radioactive [γ-^{32}P]-ATP, GSK3β and a peptide substrate of GSK3β, monitoring phosphorylation of the peptide by scintillation counting. Like the assays conducted earlier, NaSH significantly inhibited phosphorylation of the peptide (*SI Appendix*, Fig. S3B). As HEK293 cells harbor other kinases such as extracellular signal-related kinase-1 and -2, and mitogen-activated protein kinases, p38 kinase and c-jun N-terminal kinase, which can also phosphorylate Tau, it remains to be determined whether H_2S inhibits phosphorylation of Tau by these kinases (48). Thus, it appeared likely that H_2S prevents phosphorylation of Tau by inhibiting GSK3β, possibly by sulfhydrating it. Therefore we examined the sulfhydration of GSK3β using mass spectrometry, revealing that GSK3β was indeed modified by H_2S at Cys218 (*SI Appendix*, Fig. S4). A closer analysis of the sequence of

GSK3β revealed that Cys218 lies close to Tyr216 which is phosphorylated in the kinase domain. Moreover, 3D-modeling showed that Cys218 lies close to Asp181 in the active site, which is involved in hydrogen bond formation for catalysis. Persulfidation or sulfhydration of Cys218 could disrupt the active site conformation (Fig. 3*D,E*). We analyzed sulfhydration of GSK3β in human AD samples using the dimedone switch assay in combination with an antibody array method we previously developed (39). In this method, a GSK3β antibody is immobilized on a 96 well plate with an *N*-hydroxysuccinimide (NHS)-activated surface as described previously (Fig. 3*F*) (39). Considering that proteins are labelled with 4-chloro-7-nitrobenzofurazan (NBF, green) reflecting total load and with cyanine-5 (Cy5, red) for sulfhydration, the ratio of these two signals would yield the observed levels of GSK3β sulfhydration. As a negative control 488-labelled albumin (instead of antibody) was used to block the available surface and then incubated with control lysates. The assay revealed that sulfhydration of GSK3β was significantly diminished in the cortex of AD patients, as compared to normal subjects (Fig. 3*G,H*). Sulfhydration of GSK3β was decreased almost two-fold in the cerebral cortex of AD patients, further confirming our observation that sulfhydration is decreased in AD.

H_2S donors alleviate behavioral symptoms in the 3xTg-AD mouse model

To examine the neuroprotective effects of H_2S *in vivo*, we administered NaGYY, a synthetic sodium salt derivative of Lawesson's reagent, N-benzoylthiobenzamide, GYY4137 and a slow releasing H_2S donor to 3xTg-AD mice (49-52). Commercially available GYY4137 is synthesized as a morpholine salt (morpholine is toxic and biologically active) and also contains undisclosed amounts of the carcinogenic solvent (dichloromethane) which is metabolized to CO, potentially complicating the interpretation of effects obtained. Accordingly, we utilized in-house ultrapure NaGYY (See Materials and Methods for additional details), which is devoid of these confounding effects and has been well characterized with the additional advantage of being water soluble (52, 53).

Mice were treated either with NaGYY or saline (vehicle) at 6-mo via daily intraperitoneal injections (100 mg/kg in saline) for 12 wk. Levels of sulfhydration and behavioral studies were conducted 3-mo after treatment with NaGYY at 9-mo. Overall levels of sulfhydration were decreased in the 3xTg-AD mice, which was rescued in the 3xTg-AD mice treated with NaGYY (Fig. 4*A*). In addition, we observed that sulfhydration of immunoprecipitated Tau is decreased in AD mice and restored in NaGYY treated animals (Fig. 4*B*). Next, we studied the effects of the H_2S donor on motor and cognitive functions of AD mice. We used an open field test to study the overall locomotor activity of 3xTg-AD mice treated with the H_2S donor. The AD mice had a reduced locomotor activity as compared to the wild type mice. NaGYY treatment enhanced overall locomotor activity of the AD mice (Fig. 4*C*). The most studied features of AD are memory impairments and cognitive deficits,

although non-cognitive deficits, such as motor dysfunction, are also present and may even precede classical clinical symptoms (54). Motor symptoms have been observed in patients with autosomal dominant AD which correlate with disease progression (55). Treatment with NaGYY partially rescued memory deficits of 3xTg-AD mice in the Barnes maze memory tests at 9-mo as compared to their vehicle (saline)-treated controls. The primary latency in the Barnes maze test was significantly improved, but there was no significant change in the primary, total error, or total latency in these mice (Fig. 4*D-G*). Thus, the H_2S donor NaGYY elicits beneficial effects on motor and cognitive deficits of AD mice.

Discussion

The principal finding of this study is that the gasotransmitter, H_2S is neuroprotective in AD, by inhibiting phosphorylation of Tau via sulfhydration of GSK3β, the kinase for Tau. In addition, by sulfhydrating cysteine residues on target proteins, H_2S prevents irreversible oxidation of cysteine residues as demonstrated previously (39). Earlier we reported decreased H_2S signaling by sulfhydration in PD, HD and during aging (24, 25, 39). Neuronal H_2S produced by CSE mediates stress responses, which are compromised in neurodegenerative diseases (38, 56).

H_2S levels are tightly regulated in cells. Excess H_2S deranges mitochondria and has been implicated in a state of suspended animation, attributed to inhibition of complex IV of the electron transport chain (57, 58). The major H_2S-producing enzymes are spatially compartmentalized in the adult brain, with CBS concentrated in astrocytes and CSE in neurons (29, 59). In amyotrophic lateral sclerosis (ALS) caused by the G93A mutation in superoxide dismutase 1 (SOD1) and in Down's Syndrome (DS), excess H_2S is neurotoxic (60-63). H_2S donors are therapeutic in several AD models, however direct links to sulfhydration have not been established (43, 64-70).

In this study, we detected diminished expression of CSE and sulfhydration in the AD brain. The 3xTg-AD mouse model as well as postmortem cortex samples of AD patients display reduced sulfhydration. Supplementation with the slow releasing H_2S donor, NaGYY rescues the diminished sulfhydration levels in the brains of 3xTg-AD mouse model and alleviates motor and cognitive deficits. Our findings concur with reports of diminished H_2S levels in serum of AD patients and confirm the neuroprotective role of H_2S donors in rodent models of AD (42, 43, 64, 65, 69, 71, 72). Treatment with H_2S donors ameliorated several deficits including those in learning and memory.

How might sulfhydration be neuroprotective? We propose that H_2S sulfhydrates GSK3β, thereby inhibiting phosphorylation of Tau and preventing neurotoxicity (Fig. 4*H*). As H_2S participates in multiple signaling cascades, additional neuroprotective pathways may be involved (37). For example, the Nuclear factor erythroid 2-related factor 2 (Nrf2) signaling pathway, which regulates response to oxidative stress response, may be enhanced by H_2S. Under basal conditions, Nrf2 is sequestered in the cytosol of cells by the kelch-like ECH-associated protein (Keap1), which targets

it for proteasomal degradation (73). Keap1 has reactive cysteine residues, which, when sulfhydrated, causes its dissociation from Nrf2, which then translocates to the nucleus to transcribe genes involved in stress responses (42, 74). Similarly, H_2S modulates transcriptional regulatory networks which are disrupted in neurodegeneration (38, 75). Stimulating the reverse transsulfuration pathway may be beneficial in AD. This pathway also leads to the production of glutathione**,** the cellular antioxidant, which regulates redox homeostasis and neurotransmission (76, 77). As the reverse transsulfuration pathway is a central hub in several neuroprotective signaling networks, its stimulation may afford therapeutic benefits by restoring redox balance and H_2S metabolism (28, 41). This pathway is disrupted in several neurodegenerative diseases exhibiting impaired redox homeostasis. Thus in PD and HD, stimulating the production of cysteine and H_2S via CSE is neuroprotective (24, 25, 38, 56). Aging is associated with diminished transsulfuration, and sulfhydration as well as elevated oxidative stress. We have shown previously that decreased sulfhydration and increased oxidation of cysteine residues on proteins occur across evolutionary boundaries during aging (39). Additionally, aging is the greatest risk factor for developing neurodegenerative diseases including AD (78). Accordingly, targeting the reverse transsulfuration pathway may afford therapeutic benefits for aging and neurodegenerative diseases involving suboptimal H_2S signaling.

Materials and Methods

Cell cultures and reagents

HEK293 cells were from American Tissue Culture Type Collection (ATCC). All chemicals were from Sigma unless mentioned otherwise. In this study we used a sodium salt of derivative of the slow release H_2S donor, GYY4137 (NaGYY). Use of this compound was necessary, as commercial preparations of GYY4137 is a morpholine salt and complexed with unstated quantities of the carcinogenic solvent methylene chloride. Morpholine and dichloromethane (methylene chloride) are highly toxic and are not biologically inert with the latter well documented to be metabolized to carbon monoxide. Since sodium salts are pharmaceutically acceptable and non-toxic, we therefore synthesized NaGYY in-house as described previously by us to avoid these contaminants and impurities (51, 52). Lipofectamine 2000 (Invitrogen) was used for all transfection studies. The pRK5-eGFP-Tau (46904), pRK5-eGFP-Tau P301L (4690), pcDNA3-HA-GSK3β (14753), and pcDNA3-HA-GSK3β S9A (14754) constructs were obtained from Addgene.

Immunoprecipitation assays and Western blot analysis

HEK293 cells were transfected with indicated plasmids 24 h prior to lysis of the cells. Cells were lysed in buffer (IP buffer), containing 50 mM Tris·HCl (pH 8.0), 150 mM NaCl, 1% Triton X-100, 10

% glycerol protease inhibitors (cOmplete™, EDTA-free Protease Inhibitor Cocktail from Sigma) and phosphatase inhibitors (PhosSTOP™ phosphatase inhibitor, Sigma) and lysates were cleared by centrifugation at 16,000 g for 10 min followed by recovery of the supernatant. Protein was quantified by Bradford assay and samples were normalized for protein content. Inputs were reserved and 500 µg of protein was incubated with GST beads overnight at 4 °C with rotation. Beads were washed four times in IP buffer, followed by elution into 1X LDS buffer (Stock 4X containing 40% glycerol, 4% lithium dodecyl sulfate (LDS), 0.8 M triethanolamine-Cl pH 7.6, 4% Ficoll®-400, 0.025% phenol red, 0.025% Coomassie G250, 2 mM EDTA disodium from Thermo Fisher Scientific, USA) with 1 mM DTT at 95 °C for 5 min. Samples and inputs were loaded on a mini NuPAGE 4-12% Bis-Tris gel (Thermo Fisher, Scientific USA) and electrophoresed in 1X NuPAGE MES (2-(N-morpholino) ethanesulfonic acid) SDS running buffer (Thermo Fisher Scientific, USA) and immunoblotted with the indicated antibodies. Antibodies used include anti-CSE, generated in-house (36) (1: 4000), anti-FLAG (1: 3000, Sigma), anti-GST-HRP (1:10,000, Sigma), anti-Tau (1: 1000, Santa Cruz Biotechnology), anti-GFP (1:1000, Cell Signaling Technology), anti-p396Tau (1:1000, Santa Cruz Biotechnology), anti-GSK3β (1: 1000, Santa Cruz Biotechnology), anti-β-actin HRP (1:10,000, Santa Cruz Biotechnology). For the *in vitro* immunoprecipitation assays, either anti-Tau antibody or normal mouse IgG control was incubated with Protein A/G agarose overnight at 4 °C with rotation. Antibody-agarose mixture was incubated with purified wild type Tau for 6 h at 4 °C with rotation, washed three times in IP buffer, and incubated with CSE overnight at 4 °C with rotation. Beads were washed four times in IP buffer followed by elution into LDS buffer with 1 mM DTT at 95 °C for 5 min. Samples and inputs were analyzed by western blotting as described above. Additional details of reagents and methods are available in *SI Appendix*.

Acknowledgments

This work was supported by US Public Health Service Grant DA044123 (to S.H.S) and the American Heart Association (AHA)-Allen Initiative in Brain Health and Cognitive Impairment (to S.H.S and associates), Medical Research Council, UK (MR/S002626/1 to MW), the Brian Ridge Scholarship (RT), the European Research Council (ERC) under the European Union's Horizon 2020 research and innovation programme (864921 to MRF). We are grateful to Olga Pletnikova, Brain Resource Center (BRC) at Johns Hopkins University for providing post-mortem AD brain samples. The Johns Hopkins University Mass Spectrometry Core is acknowledged for analysis of protein sulfhydration. We especially thank the reviewers for their valuable comments and suggestions, which have greatly strengthened the study.

Author disclosures

MW, RT and the University of Exeter have patents (awarded/pending) on hydrogen sulfide delivery molecules and their therapeutic use.

Figure Legends

Fig. 1. Cystathionine γ-lyase expression is decreased in Alzheimer's disease. (*A*) The reverse transsulfuration pathway in mammals. Homocysteine, generated from dietary methionine, is condensed with serine to generate cystathionine by cystathionine β-synthase (CBS). Cystathionine is acted on by cystathionine γ-lyase (CSE) to produce cysteine. Cysteine can either be utilized to synthesize glutathione and other sulfur containing molecules or used as a substrate to generate hydrogen sulfide (H_2S). Both homocysteine and cysteine may be utilized to produce H_2S. While CSE may generate H_2S from either cysteine or homocysteine, CBS produces H_2S using a combination of cysteine and homocysteine. 3-mercaptopyruvate sulfur transferase (3-MST), in conjunction with cysteine amino transferase (CAT), a third enzyme, also produces H_2S from cysteine. (*B*) CSE is depleted in the cortex of 24-mo 3xTg-AD mice. *n*=3, SEM, **P* < 0.05. (*C*) CSE is depleted in the hippocampus of 3xTg-AD mice. *n*=3, SEM, **P* < 0.05. (*D*) CSE is diminished in the cortex of AD patients (Braak stage 6). *n*=3, SEM, **P* < 0.05. (*E)* The dimedone switch assay. Proteins were reacted with 4-chloro-7-nitrobenzofurazan (NBF-Cl), to label persulfides, thiols, sulfenic acids, and amino groups. Reaction with amino groups specifically results in a characteristic green fluorescence. Next, the NBF tag is switched by a dimedone-based probe, which emits red fluorescence (the Cy5 tag is shown as a red circle), selectively labeling persulfides. The mixture is then run on SDS gels and signals detected by fluorescence scanning. (*F*) Gel scan showing reduced sulfhydration in postmortem human AD brain samples and quantitation. *n*=4, SEM **P* < 0.05.

Fig. 2. Cystathionine γ-lyase (CSE) binds the microtubule binding protein Tau. (*A*) Schematic representation of full-length Tau, which is composed of 441 amino acids. Tau harbors the N terminal domains, N1 and N2, a proline-rich region (PRR) and four repeat domains R1 through R4 which bind microtubules. Two cysteine residues Cys291 and Cys322 are present in R2 and R3 respectively. (*B*) Interaction of Tau with CSE and CBS. HEK293 cells were transfected with constructs encoding Flag tagged wild type Tau (Flag-Tau) and either GST tagged CSE or CBS or GST vector and GST pulldown assay conducted. GST-CSE and GST-CBS interact with Flag-Tau. (*C*) CSE binds Tau directly. *In vitro* coimmunoprecipitation assay using purified CSE and Tau. Normal IgG control was used as an isotype control for the anti-Tau antibody used in the immunoprecipitation. (*D*) CSE and CBS do not bind to mutant Tau P301L as revealed by co-immunoprecipitation assays in HEK293 cells overexpressing GST-CSE or GST-CBS and either

wild type Tau (WT) or mutant Tau P301L. Arrow with "s" indicates specific GFP-Tau band, arrow with "ns" indicates non-specific band. (*E*) Wild type Tau stimulates activity of CSE *in vitro* (using purified proteins) as measured by H_2S production by the methylene blue assay. *n*=3, SEM, **P* < 0.05. (*F*) Kinetics of H_2S production from human recombinant CSE without (black squares) or with Tau (red dots). CSE/Tau protein molar ratio is ½. Wild type Tau stimulates activity of CSE as assayed by a spectrophotometric assay utilizing 0.22 μM purified CSE and 0.44 μM in 100 mM HEPES buffer (pH 7.4) containing 0.4 mM lead acetate at 37 °C for 3 min and absorbance measured at 390 nm, reflecting the formation lead sulfide formed by reaction of H_2S with lead acetate. (*G*) Wild type Tau stimulates activity of CSE in HEK 293 cells in an *in vitro* reaction containing 10 mM L-cysteine and 250 μM pyridoxal 5-phosphate (PLP) as measured by H_2S production by the methylene blue assay. *n*=3, SEM, ***P* < 0.01. (*H*) WT Tau increases the activity of CSE in a time dependent manner. *n*=3, SEM, ****P* < 0.001. (*I*) Tau is sulfhydrated by H_2S. Flag-Tau was transfected into HEK293 and treated with 100 μM NaSH and sulfhydration analyzed by the modified biotin switch assay.

Fig. 3. CSE and H_2S inhibit phosphorylation of Tau by GSK3β. (*A*) Phosphorylation assays with purified Tau, GSK3β and CSE *in vitro*, in the presence or absence of L-cysteine (L-cys) and pyridoxal 5'-phosphate (PLP) or treated with 100 μM NaSH. Phosphorylation of Tau was assessed by western blotting using antibodies against phosphorylated Tau (pTau 396). Tau phosphorylation was significantly diminished when CSE, L-cysteine and PLP were added. Addition of NaSH alone, in the absence of CSE also prevented Tau phosphorylation. (*B*) Cysteine residues do not play a role in phosphorylation of Tau by GSK3β. Purified Tau or Tau C291S/C322S and GSK3β were incubated in the presence or absence of L-cysteine and PLP and analyzed for phosphorylation of Tau at Ser396. Western blot analysis revealed that mutation of cysteine residues Cys291 and Cys322 does not affect phosphorylation of Tau at Ser396. *n*=3, SEM, **P* <0.05, ****P* < 0.001. (*C*) H_2S inhibits phosphorylation of P301L Tau by GSK3β. HEK293 cells were transfected with Tau P301L or Tau P301L C291S/C322S and GSK3β S9A and treated with 100 μM NaSH for 24 h and analyzed for phosphorylation of Tau at Ser396 by western blotting. While GSK3β phosphorylated Tau, NaSH prevented this phosphorylation. (*D*) Ribbon Model of GSK3β (PDB:1j1b; DOI: 10.1107/S090744490302938X). Intercept: (*E*) Thiolate side chain of Cys218 (ball and stick model), that we found to be sulfhydrated, is already in a close proximity to Asp181 in the active site of GSK3β, so the presence of an additional sulfur atom will inevitably alter the conformation of the active site, which would inhibit its kinase activity. Oxygen atoms are shown in red, sulfur in yellow and nitrogen in blue. Dots around the atoms represent expected water surface accessibility. (*F*) Schematic representation of the antibody array-like approach to study sulfhydration status of GSK3β in AD brains. Anti-GSK3β antibody was immobilized on a 96 well plate with NHS-activated

surface. Brain cortical lysates from normal and AD post-mortem tissues were added to the wells to allow recognition of GSK3β from lysates by the antibody. The bound protein was labeled with NBF (green) for a total load and with Cy5 (red) for sulfhydration and the ratio of the two signals measured to yield sulfhydration levels. As a negative control 488-labelled albumin (instead of antibody) was used to block the available surface and then incubated with control lysates. (*G*) Read-out from a representative experiment showing decreased sulfhydration (red) in cortex of AD patients, while the negative control shows no signals. The plate was recorded on Typhoon FL9500 at 488 nm (NBF fluorescence signal, green, which represents total load) and 635 nm (Cy5 signal (red), which represents sulfhydration). (*H*) Quantitation of *H. n*=4, SEM, ***$P < 0.001$.

Fig. 4. The H_2S donor, NaGYY ameliorates AD symptoms. (*A*) Overall sulfhydration is decreased in the hippocampus of 3xTg-AD mice, which is rescued by NaGYY treatment in 3xTg-AD mice as revealed by the dimedone switch method. *n*=3, SEM, ***$P < 0.001$. (*B*) Sulfhydration of Tau is decreased in the hippocampus of 3xTg-AD mice as revealed by immunoprecipitation assays in combination with the dimedone switch assay. Treatment with NaGYY rescues sulfhydration of Tau. (*C*) Treatment regimen for 3xTg-AD mice with the H_2S donor, NaGYY. Mice were treated at 6-mo with 100 mg/kg NaGYY by intraperitoneal injection daily for 12 wk and behavioral analyses conducted at 9-mo. The open field test revealed significant deficits in locomotor activity in the male 3xTg-AD mice, which were rescued by NaGYY. *n*=6-10, SEM, **$P < 0.01$ and *$P < 0.05$. (*D-G*) NaGYY partially rescues memory deficits in the 3xTg-AD mice. These mice do not exhibit significant differences in primary error and total error in the Barnes Maze test (*D,E*). NaGYY treatment partially rescues primary and total latency (*F,G*). *n*=6-10, SEM, *$P < 0.05$ for comparison between primary latency of 3xTg-AD Saline and 3xTg-AD NaGYY by one-way ANOVA followed by a post-hoc Tukey test. (*H*) Model depicting a possible mode of neuroprotection afforded by H_2S. GSK3β (yellow-ochre) binds Tau (purple) and phosphorylates it (depicted as “P”), which leads to the formation of neurofibrillary tangles (NFTs) and AD pathology in the 3xTgAD mice. H_2S produced by CSE (green) sulfhydrates GSK3β (“SH” in red text) and inhibits phosphorylation of Tau. Tau binds to CSE and enhances its activity (arrow with a “+” sign), forming part of a virtuous cycle that decreases Tau phosphorylation and confers neuroprotection.

References

1. C. A. Lane, J. Hardy, J. M. Schott, Alzheimer's disease. *Eur J Neurol* **25**, 59-70 (2018).
2. C. L. Masters *et al.*, Alzheimer's disease. *Nat Rev Dis Primers* **1**, 15056 (2015).
3. J. M. Long, D. M. Holtzman, Alzheimer Disease: An Update on Pathobiology and Treatment Strategies. *Cell* **179**, 312-339 (2019).

4. J. L. Cummings, T. Morstorf, K. Zhong, Alzheimer's disease drug-development pipeline: few candidates, frequent failures. *Alzheimers Res Ther* **6**, 37 (2014).
5. C. M. Karch, A. M. Goate, Alzheimer's disease risk genes and mechanisms of disease pathogenesis. *Biol Psychiatry* **77**, 43-51 (2015).
6. C. Ballatore, V. M. Lee, J. Q. Trojanowski, Tau-mediated neurodegeneration in Alzheimer's disease and related disorders. *Nat Rev Neurosci* **8**, 663-672 (2007).
7. V. M. Lee, M. Goedert, J. Q. Trojanowski, Neurodegenerative tauopathies. *Annu Rev Neurosci* **24**, 1121-1159 (2001).
8. T. Arendt, J. T. Stieler, M. Holzer, Tau and tauopathies. *Brain Res Bull* **126**, 238-292 (2016).
9. M. D. Weingarten, A. H. Lockwood, S. Y. Hwo, M. W. Kirschner, A protein factor essential for microtubule assembly. *Proc Natl Acad Sci U S A* **72**, 1858-1862 (1975).
10. J. Avila, J. J. Lucas, M. Perez, F. Hernandez, Role of tau protein in both physiological and pathological conditions. *Physiol Rev* **84**, 361-384 (2004).
11. T. Arakhamia *et al.*, Posttranslational Modifications Mediate the Structural Diversity of Tauopathy Strains. *Cell* **180**, 633-644 e612 (2020).
12. Y. Wang, E. Mandelkow, Tau in physiology and pathology. *Nat Rev Neurosci* **17**, 5-21 (2016).
13. L. Martin, X. Latypova, F. Terro, Post-translational modifications of tau protein: implications for Alzheimer's disease. *Neurochem Int* **58**, 458-471 (2011).
14. H. Braak, E. Braak, Staging of Alzheimer's disease-related neurofibrillary changes. *Neurobiol Aging* **16**, 271-278; discussion 278-284 (1995).
15. T. Gomez-Isla *et al.*, Neuronal loss correlates with but exceeds neurofibrillary tangles in Alzheimer's disease. *Ann Neurol* **41**, 17-24 (1997).
16. M. Medina, F. Hernandez, J. Avila, New Features about Tau Function and Dysfunction. *Biomolecules* **6** (2016).
17. M. Jouanne, S. Rault, A. S. Voisin-Chiret, Tau protein aggregation in Alzheimer's disease: An attractive target for the development of novel therapeutic agents. *Eur J Med Chem* **139**, 153-167 (2017).
18. G. Lindwall, R. D. Cole, Phosphorylation affects the ability of tau protein to promote microtubule assembly. *J Biol Chem* **259**, 5301-5305 (1984).
19. I. Grundke-Iqbal *et al.*, Abnormal phosphorylation of the microtubule-associated protein tau (tau) in Alzheimer cytoskeletal pathology. *Proc Natl Acad Sci U S A* **83**, 4913-4917 (1986).
20. B. R. Hoover *et al.*, Tau mislocalization to dendritic spines mediates synaptic dysfunction independently of neurodegeneration. *Neuron* **68**, 1067-1081 (2010).
21. J. I. Sbodio, S. H. Snyder, B. D. Paul, Redox Mechanisms in Neurodegeneration: From Disease Outcomes to Therapeutic Opportunities. *Antioxid Redox Signal* **30**, 1450-1499 (2019).
22. V. Vitvitsky, M. Thomas, A. Ghorpade, H. E. Gendelman, R. Banerjee, A functional transsulfuration pathway in the brain links to glutathione homeostasis. *J Biol Chem* **281**, 35785-35793 (2006).
23. L. Diwakar, V. Ravindranath, Inhibition of cystathionine-gamma-lyase leads to loss of glutathione and aggravation of mitochondrial dysfunction mediated by excitatory amino acid in the CNS. *Neurochem Int* **50**, 418-426 (2007).
24. B. D. Paul *et al.*, Cystathionine gamma-lyase deficiency mediates neurodegeneration in Huntington's disease. *Nature* **509**, 96-100 (2014).
25. M. S. Vandiver *et al.*, Sulfhydration mediates neuroprotective actions of parkin. *Nat Commun* **4**, 1626 (2013).
26. J. B. Kohl, A. T. Mellis, G. Schwarz, Homeostatic impact of sulfite and hydrogen sulfide on cysteine catabolism. *Br J Pharmacol* **176**, 554-570 (2019).
27. N. Sen *et al.*, Hydrogen sulfide-linked sulfhydration of NF-kappaB mediates its antiapoptotic actions. *Mol Cell* **45**, 13-24 (2012).

28. J. I. Sbodio, S. H. Snyder, B. D. Paul, Regulators of the transsulfuration pathway. *Br J Pharmacol* **176**, 583-593 (2019).
29. T. Morikawa *et al.*, Hypoxic regulation of the cerebral microcirculation is mediated by a carbon monoxide-sensitive hydrogen sulfide pathway. *Proc Natl Acad Sci U S A* **109**, 1293-1298 (2012).
30. B. D. Paul, S. H. Snyder, H2S: A Novel Gasotransmitter that Signals by Sulfhydration. *Trends Biochem Sci* **40**, 687-700 (2015).
31. B. D. Paul, S. H. Snyder, Protein sulfhydration. *Methods Enzymol* **555**, 79-90 (2015).
32. B. D. Paul, S. H. Snyder, H(2)S signalling through protein sulfhydration and beyond. *Nat Rev Mol Cell Biol* **13**, 499-507 (2012).
33. M. R. Filipovic, J. Zivanovic, B. Alvarez, R. Banerjee, Chemical Biology of H2S Signaling through Persulfidation. *Chem Rev* **118**, 1253-1337 (2018).
34. R. Wang, Physiological implications of hydrogen sulfide: a whiff exploration that blossomed. *Physiol Rev* **92**, 791-896 (2012).
35. R. Wang, Hydrogen sulfide: a new EDRF. *Kidney Int* **76**, 700-704 (2009).
36. G. Yang *et al.*, H2S as a physiologic vasorelaxant: hypertension in mice with deletion of cystathionine gamma-lyase. *Science* **322**, 587-590 (2008).
37. B. D. Paul, S. H. Snyder, Gasotransmitter hydrogen sulfide signaling in neuronal health and disease. *Biochem Pharmacol* **149**, 101-109 (2018).
38. J. I. Sbodio, S. H. Snyder, B. D. Paul, Transcriptional control of amino acid homeostasis is disrupted in Huntington's disease. *Proc Natl Acad Sci U S A* **113**, 8843-8848 (2016).
39. J. Zivanovic *et al.*, Selective Persulfide Detection Reveals Evolutionarily Conserved Antiaging Effects of S-Sulfhydration. *Cell Metab* **30**, 1152-1170 e1113 (2019).
40. W. Droge, Oxidative stress and ageing: is ageing a cysteine deficiency syndrome? *Philos Trans R Soc Lond B Biol Sci* **360**, 2355-2372 (2005).
41. B. D. Paul, J. I. Sbodio, S. H. Snyder, Cysteine Metabolism in Neuronal Redox Homeostasis. *Trends Pharmacol Sci* **39**, 513-524 (2018).
42. Y. Liu *et al.*, Hydrogen sulfide ameliorates learning memory impairment in APP/PS1 transgenic mice: A novel mechanism mediated by the activation of Nrf2. *Pharmacol Biochem Behav* **150-151**, 207-216 (2016).
43. A. Xuan *et al.*, Hydrogen sulfide attenuates spatial memory impairment and hippocampal neuroinflammation in beta-amyloid rat model of Alzheimer's disease. *J Neuroinflammation* **9**, 202 (2012).
44. S. Oddo *et al.*, Triple-transgenic model of Alzheimer's disease with plaques and tangles: intracellular Abeta and synaptic dysfunction. *Neuron* **39**, 409-421 (2003).
45. H. Takuma, S. Arawaka, H. Mori, Isoforms changes of tau protein during development in various species. *Brain Res Dev Brain Res* **142**, 121-127 (2003).
46. P. McMillan *et al.*, Tau isoform regulation is region- and cell-specific in mouse brain. *J Comp Neurol* **511**, 788-803 (2008).
47. D. P. Hanger, B. H. Anderton, W. Noble, Tau phosphorylation: the therapeutic challenge for neurodegenerative disease. *Trends Mol Med* **15**, 112-119 (2009).
48. B. H. Anderton *et al.*, Sites of phosphorylation in tau and factors affecting their regulation. *Biochem Soc Symp* 10.1042/bss0670073, 73-80 (2001).
49. Y. Zhao, H. Wang, M. Xian, Cysteine-activated hydrogen sulfide (H_2S) donors. *J Am Chem Soc* **133**, 15-17 (2011).
50. L. Li *et al.*, Characterization of a novel, water-soluble hydrogen sulfide-releasing molecule (GYY4137): new insights into the biology of hydrogen sulfide. *Circulation* **117**, 2351-2360 (2008).
51. M. Whiteman *et al.*, Phosphinodithioate and Phosphoramidodithioate Hydrogen Sulfide Donors. *Handb Exp Pharmacol* **230**, 337-363 (2015).
52. B. E. Alexander *et al.*, Investigating the generation of hydrogen sulfide from the phosphonamidodithioate slow-release donor GYY4137. *MedChemComm* **6**, 1649-1655 (2015).

53. E. Latorre, R. Torregrossa, M. E. Wood, M. Whiteman, L. W. Harries, Mitochondria-targeted hydrogen sulfide attenuates endothelial senescence by selective induction of splicing factors HNRNPD and SRSF2. *Aging (Albany NY)* **10**, 1666-1681 (2018).
54. J. M. Wagner *et al.*, Analysis of Motor Function in the Tg4-42 Mouse Model of Alzheimer's Disease. *Front Behav Neurosci* **13**, 107 (2019).
55. J. Voglein *et al.*, Clinical, pathophysiological and genetic features of motor symptoms in autosomal dominant Alzheimer's disease. *Brain* **142**, 1429-1440 (2019).
56. J. I. Sbodio, S. H. Snyder, B. D. Paul, Golgi stress response reprograms cysteine metabolism to confer cytoprotection in Huntington's disease. *Proc Natl Acad Sci U S A* **115**, 780-785 (2018).
57. E. Blackstone, M. Morrison, M. B. Roth, H2S induces a suspended animation-like state in mice. *Science* **308**, 518 (2005).
58. B. D. Paul, S. H. Snyder, K. Kashfi, Effects of hydrogen sulfide on mitochondrial function and cellular bioenergetics. *Redox Biol* **38**, 101772 (2020).
59. Y. Enokido *et al.*, Cystathionine beta-synthase, a key enzyme for homocysteine metabolism, is preferentially expressed in the radial glia/astrocyte lineage of developing mouse CNS. *FASEB J* **19**, 1854-1856 (2005).
60. A. Ichinohe *et al.*, Cystathionine beta-synthase is enriched in the brains of Down's patients. *Biochem Biophys Res Commun* **338**, 1547-1550 (2005).
61. T. Panagaki, E. B. Randi, F. Augsburger, C. Szabo, Overproduction of H_2S, generated by CBS, inhibits mitochondrial Complex IV and suppresses oxidative phosphorylation in Down syndrome. *Proc Natl Acad Sci U S A* **116**, 18769-18771 (2019).
62. A. Davoli *et al.*, Evidence of hydrogen sulfide involvement in amyotrophic lateral sclerosis. *Ann Neurol* **77**, 697-709 (2015).
63. P. Kamoun, M. C. Belardinelli, A. Chabli, K. Lallouchi, B. Chadefaux-Vekemans, Endogenous hydrogen sulfide overproduction in Down syndrome. *Am J Med Genet A* **116A**, 310-311 (2003).
64. D. Giuliani *et al.*, Hydrogen sulfide slows down progression of experimental Alzheimer's disease by targeting multiple pathophysiological mechanisms. *Neurobiol Learn Mem* **104**, 82-91 (2013).
65. E. Vandini *et al.*, Mechanisms of Hydrogen Sulfide against the Progression of Severe Alzheimer's Disease in Transgenic Mice at Different Ages. *Pharmacology* **103**, 50-60 (2019).
66. X. L. He *et al.*, Hydrogen sulfide improves spatial memory impairment and decreases production of Abeta in APP/PS1 transgenic mice. *Neurochem Int* **67**, 1-8 (2014).
67. F. L. Zhao *et al.*, AP39, a Mitochondria-Targeted Hydrogen Sulfide Donor, Supports Cellular Bioenergetics and Protects against Alzheimer's Disease by Preserving Mitochondrial Function in APP/PS1 Mice and Neurons. *Oxid Med Cell Longev* **2016**, 8360738 (2016).
68. M. M. Hu *et al.*, Sumoylation Promotes the Stability of the DNA Sensor cGAS and the Adaptor STING to Regulate the Kinetics of Response to DNA Virus. *Immunity* **45**, 555-569 (2016).
69. X. J. Cheng *et al.*, Tacrine-Hydrogen Sulfide Donor Hybrid Ameliorates Cognitive Impairment in the Aluminum Chloride Mouse Model of Alzheimer's Disease. *ACS Chem Neurosci* **10**, 3500-3509 (2019).
70. X. L. He *et al.*, Hydrogen sulfide down-regulates BACE1 and PS1 via activating PI3K/Akt pathway in the brain of APP/PS1 transgenic mouse. *Pharmacol Rep* **68**, 975-982 (2016).
71. L. Cao *et al.*, Hydrogen sulfide inhibits ATP-induced neuroinflammation and Abeta1-42 synthesis by suppressing the activation of STAT3 and cathepsin S. *Brain Behav Immun* **73**, 603-614 (2018).
72. R. Guzman *et al.*, Protective effect of sulfurous water in peripheral blood mononuclear cells of Alzheimer's disease patients. *Life Sci* **132**, 61-67 (2015).
73. J. D. Hayes, A. T. Dinkova-Kostova, The Nrf2 regulatory network provides an interface between redox and intermediary metabolism. *Trends Biochem Sci* **39**, 199-218 (2014).

74. G. Yang *et al.*, Hydrogen sulfide protects against cellular senescence via S-sulfhydration of Keap1 and activation of Nrf2. *Antioxid Redox Signal* **18**, 1906-1919 (2013).
75. A. Kumar, M. Vaish, R. R. Ratan, Transcriptional dysregulation in Huntington's disease: a failure of adaptive transcriptional homeostasis. *Drug Discov Today* **19**, 956-962 (2014).
76. T. W. Sedlak *et al.*, The glutathione cycle shapes synaptic glutamate activity. *Proc Natl Acad Sci U S A* **116**, 2701-2706 (2019).
77. H. J. Forman, H. Zhang, A. Rinna, Glutathione: overview of its protective roles, measurement, and biosynthesis. *Mol Aspects Med* **30**, 1-12 (2009).
78. Y. Hou *et al.*, Ageing as a risk factor for neurodegenerative disease. *Nat Rev Neurol* **15**, 565-581 (2019).

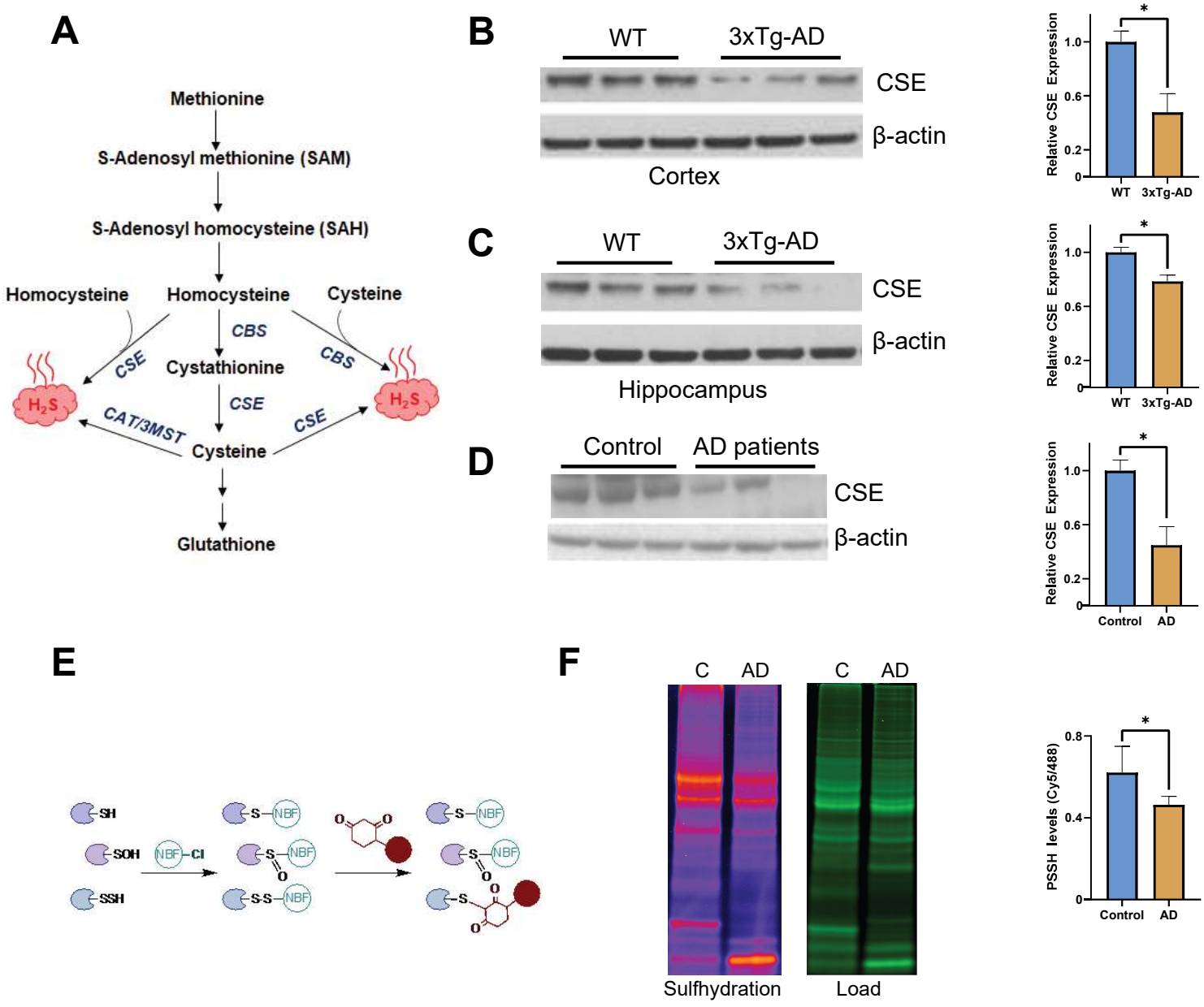
A
Methionine
S-Adenosyl methionine (SAM)
S-Adenosyl homocysteine (SAH)
Homocysteine
Homocysteine
Cysteine
CBS
CSE
CBS
Cystathionine
H_2S
H_2S
CSE
CAT/3MST
CSE
Cysteine
Glutathione
B
WT
3xTg-AD
CSE
β-actin
Cortex
Relative CSE Expression
1.0
0.6
0.2
0
*
WT
3xTg-AD
C
WT
3xTg-AD
CSE
β-actin
Hippocampus
Relative CSE Expression
1.0
0.6
0.2
0
*
WT
3xTg-AD
D
Control
AD patients
CSE
β-actin
Relative CSE Expression
1.0
0.6
0.2
0
*
Control
AD
E
SH
SOH
SSH
NBF-Cl
S-NBF
S-NBF
S-S-NBF
S-NBF
S-NBF
S-NBF
F
C
AD
C
AD
Sulfhydration
Load
PSSH levels (Cy5/488)
0.8
0.4
0
*
Control
AD

Figure 1

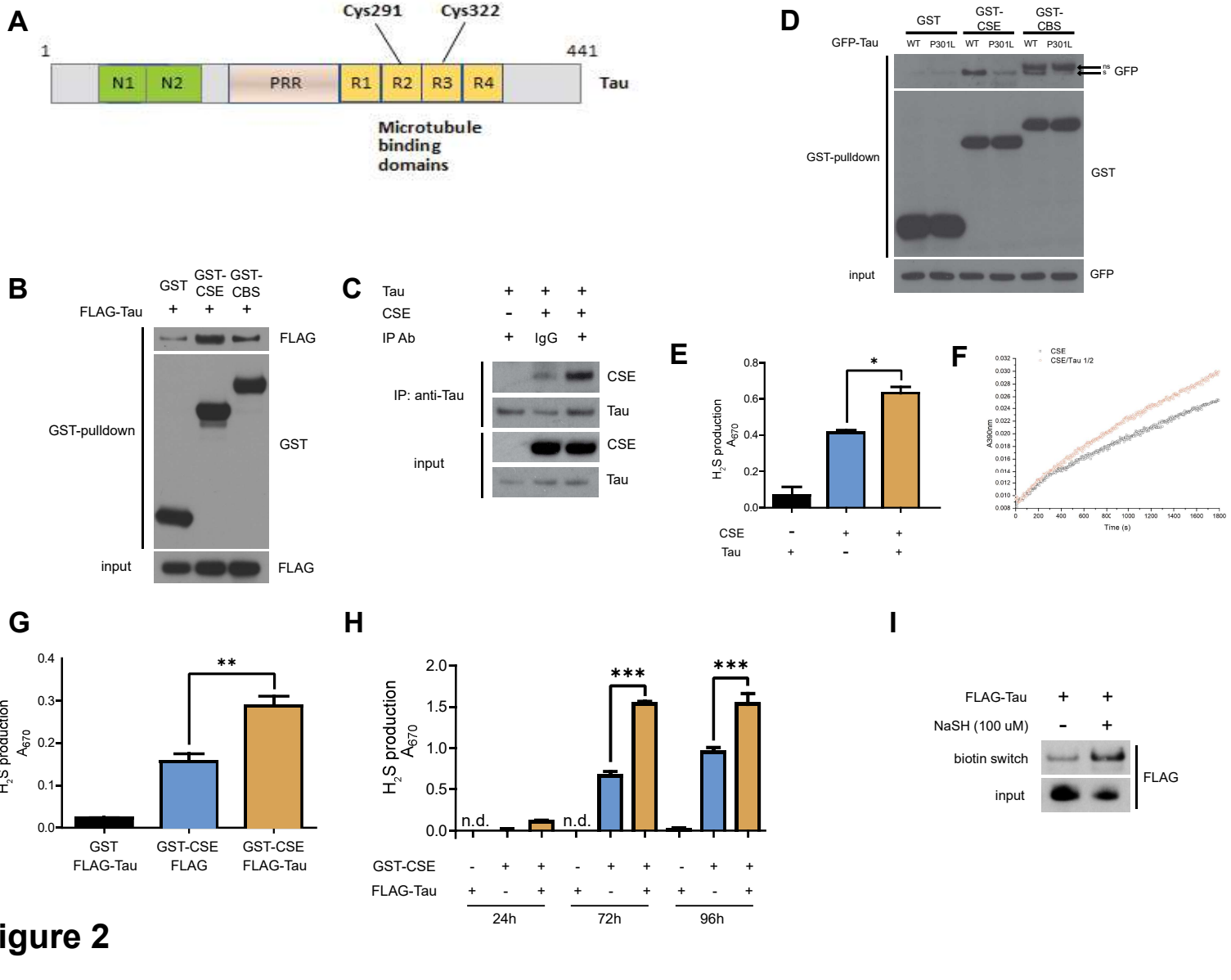
A
Cys291
Cys322
1
441
N1
N2
PRR
R1
R2
R3
R4
Tau
Microtubule binding domains
B
GST
GST-CSE
GST-CBS
FLAG-Tau
FLAG
GST-pulldown
GST
input
FLAG
C
Tau
CSE
IP Ab
IgG
IP: anti-Tau
CSE
Tau
input
CSE
Tau
D
GST
GST-CSE
GST-CBS
WT
P301L
GFP-Tau
GFP
GST-pulldown
GST
input
GFP
E
H2S production A670
CSE
Tau
F
CSE
CSE/Tau 1/2
A360nm
Time (s)
G
H2S production A670
GST FLAG-Tau
GST-CSE FLAG
GST-CSE FLAG-Tau
H
H2S production A670
n.d.
n.d.
GST-CSE
FLAG-Tau
24h
72h
96h
I
FLAG-Tau
NaSH (100 uM)
biotin switch
input
FLAG

Figure 2

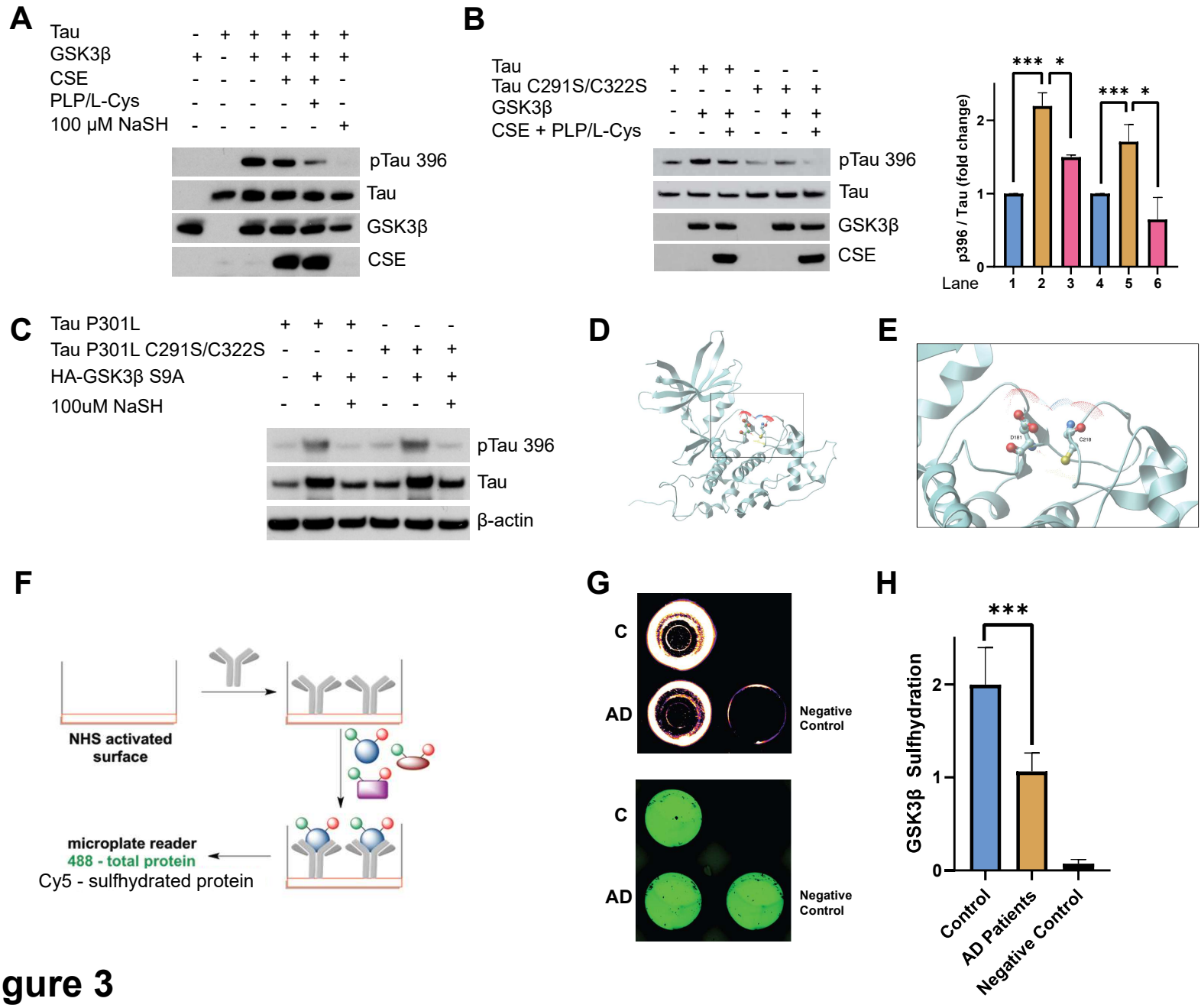
A
Tau - + + + + +
GSK3β + - + + + +
CSE - - - + + -
PLP/L-Cys - - - - + -
100 μM NaSH - - - - - +
pTau 396
Tau
GSK3β
CSE
B
Tau + + + - - -
Tau C291S/C322S - - - + + +
GSK3β - + + - + +
CSE + PLP/L-Cys - - + - - +
pTau 396
Tau
GSK3β
CSE
p396 / Tau (fold change)
Lane 1 2 3 4 5 6
C
Tau P301L + + + - - -
Tau P301L C291S/C322S - - - + + +
HA-GSK3β S9A - + + - + +
100uM NaSH - - + - - +
pTau 396
Tau
β-actin
D
E
F
NHS activated surface
microplate reader
488 - total protein
Cy5 - sulfhydrated protein
G
C
AD
Negative Control
C
AD
Negative Control
H
GSK3β Sulfhydration
Control
AD Patients
Negative Control

Figure 3

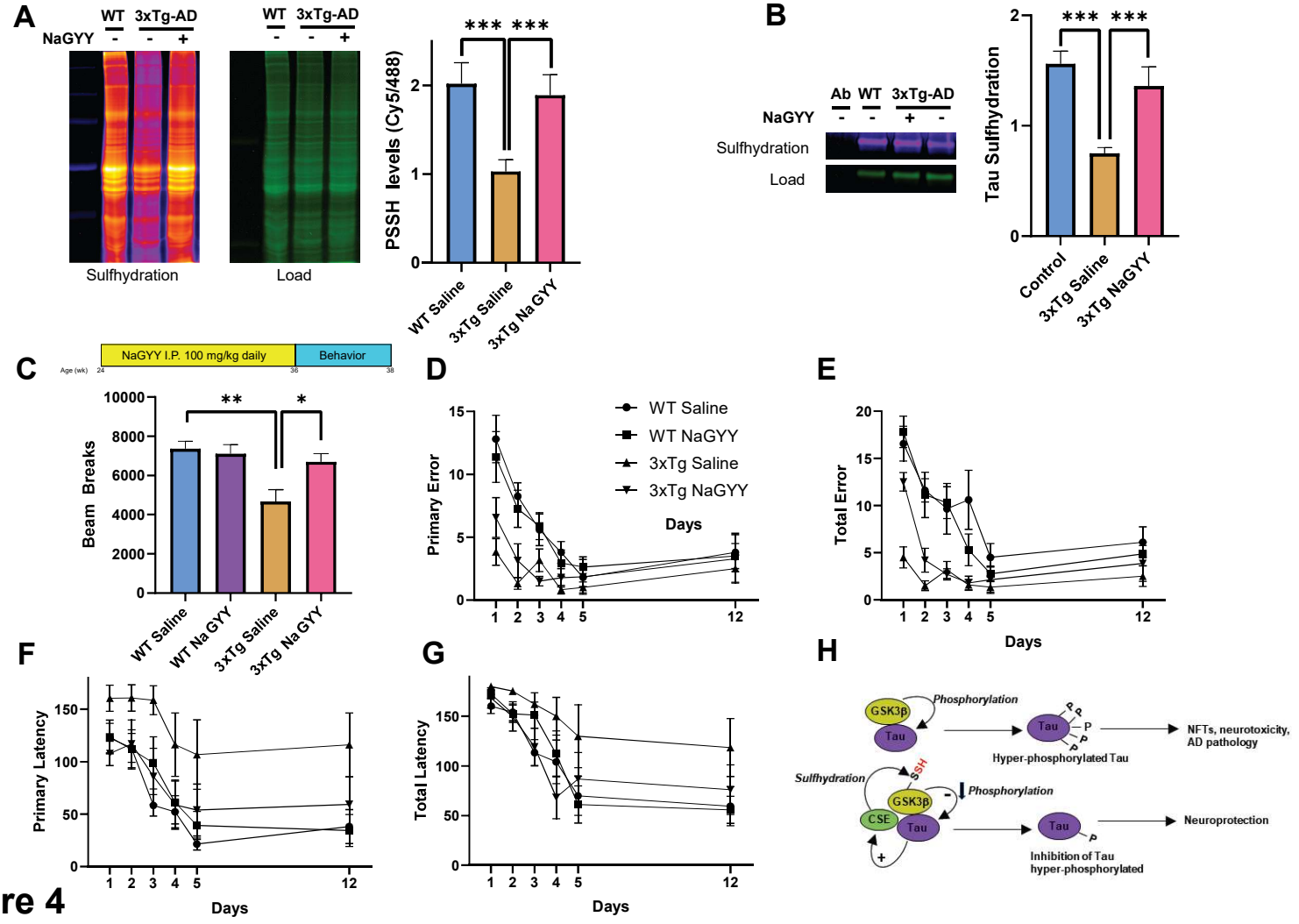
A
WT
3xTg-AD
NaGYY
- - +
Sulfhydration
Load
PSSH levels (Cy5/488)
*** ***
WT Saline
3xTg Saline
3xTg NaGYY
B
Ab WT 3xTg-AD
NaGYY
Sulfhydration
Load
Tau Sulfhydration
Control
3xTg Saline
3xTg NaGYY
C
NaGYY I.P. 100 mg/kg daily
Behavior
Age (wk)
Beam Breaks
WT Saline
WT Na GYY
3xTg Saline
3xTg Na GYY
D
WT Saline
WT NaGYY
3xTg Saline
3xTg NaGYY
Primary Error
Days
E
Total Error
Days
F
Primary Latency
Days
G
Total Latency
Days
H
GSK3β
Tau
Phosphorylation
Hyper-phosphorylated Tau
NFTs, neurotoxicity,
AD pathology
Sulfhydration
SSH
CSE
Inhibition of Tau
hyper-phosphorylated
Neuroprotection

Figure 4

PNAS
www.pnas.org

Supplementary Information for

Hydrogen sulfide is neuroprotective in Alzheimer's disease by sulfhydrating GSK3β and inhibiting Tau hyperphosphorylation.

Daniel Giovinazzo[1], Biljana Bursac[5], Juan I Sbodio[1], Sumedha Nalluru[1], Thibaut Vignane[5], Adele M. Snowman[1], Lauren M. Albacarys[1], Thomas W. Sedlak[2], Roberta Torregrossa[4], Matthew Whiteman[4], Milos R. Filipovic[5], Solomon H. Snyder[1,2,3]* and Bindu D. Paul[1]*

*Solomon H. Snyder; *Bindu D. Paul
Email: ssnyder@jhmi.edu
bpaul8@jhmi.edu

This PDF file includes:

Supplementary Information Text

Materials and Methods

Use of the H_2S donor, NaGYY

In this study we have used a sodium salt of an established H_2S generating molecule, GYY4137, NaGYY (1, 2). The reasons for this were due to confounding chemicals present in commercial sources of GYY4137, sold through all major research chemical suppliers is a morpholine salt, present at a 1:1 ratio with the parent compound. However, morpholine itself is biologically active and highly toxic with a well characterized toxicity profile, and LD50 at doses commonly used for GYY4137 (e.g. 200-400 mg/kg i.p.; http://www.inchem.org/documents/ehc/ehc/ehc179.htm). As such its presence would confound interpretation of results generated. In addition, commercial GYY4137 contains an undisclosed amount of carcinogenic solvent (dichloromethane) present as part of the crystal lattice structure (as $xCHCl_2$) and it is well known to be metabolized to carbon monoxide *in vivo*. This is particularly complicated since the CO and H_2S have similar pharmacological properties and it is possible that many of the reported effects of commercially sourced GYY4137 *in vivo* may be due to CO rather than H_2S. Moreover, with undisclosed amounts of dichloromethane (at least 0.5 molecules per molecule of GYY4137 (2), the molecular mass of commercial compound is not accurate e.g. molecular weight of commercial GYY4137 is 376.6 with additional unknown quantities of dichlromethane mwt-84.9 (so an additional 22% to the final mass. For these reasons, we have used the pharmaceutically more acceptable sodium salt which is devoid of these confounding chemicals (2, 3). The decomposition (hydrolysis) pathway and H_2S generation are identical and both salts are freely water soluble which offer considerable advantages over H_2S releasing molecules which require organic solvents such as DMSO or ethanol (themselves biologically active) such as dithiolethione and thiohyrdoxybenzamide derivatives (1, 2).

Animals and treatment

The 3xTg-AD mouse model was obtained from Jackson laboratories (Bar Harbor, Maine). Animals were housed on a 12-h light–dark schedule and received food and water ad libitum.6-mo old 3xTg-AD mice and their wild type controls were injected with either 100 mg/kg NaGYY or vehicle (saline) intraperitoneally for 12 wk and behavioral studies conducted at 9-mo.

Post-mortem brain samples

Post-mortem samples from normal and AD patients (Braak stage 6) were obtained from the Johns Hopkins Brain Center from J. Troncoso and O. Pletnikova.

Hydrogen sulfide production assays

HEK293 cells were transfected with indicated plasmids for the indicated time periods. For experiments with purified protein, purified recombinant CSE and Tau was used. Lysates or purified proteins were incubated for 6 h at 37 °C purged with nitrogen in 100 mM K+ PBS, .5% Triton X-100, 50 μM pyridoxal phosphate, 10 mM cysteine. Samples were injected with 125 μL 1% zinc acetate and 2.5 μL 10 N NaOH and incubated shaking at RT for 1 h. 500 μL of deionized water, 100 μL 20 mM N-N-dimethyl-p-phenylenediamine sulfate in 7.2M HCl, and 100 μL 30 mM $FeCl_3$ in 1.2M HCl were added to each sample and absorbance at 670 nm was subsequently measured. In addition, production of H_2S by CSE was measured in a spectrophotometric assay in which the reaction of H_2S with lead acetate to form lead sulfide was monitored at 390nm (4). Reaction buffer contained 1 mM of cysteine and 0.4 mM lead acetate in HEPES buffer (50 mM, pH 7.4) at 37 °C. hCSE (0.22 μM) or hCSE/hTau (0.22 μM/0.44 μM) were preincubated for 5 minutes at 37 °C (to allow the interaction and activation of the enzyme) before they were added into the buffer. H_2S production was monitored for 30 minutes by measuring the absorbance spectrum every 4 seconds. The reaction between lead acetate and L-cysteine in HEPES buffer was used as a control.

Sulfhydration/persulfidation assays

Sulfhydration assays were conducted using the modified biotin switch assay, the dimedone switch assay and by mass spectrometry as described previously (5-7). Briefly, HEK293 cells were transfected with wild type Tau for 24 h and treated with 100 μM NaSH for 24 h, as indicated. Cells were lysed in HEN buffer (250 mM HEPES–NaOH, pH 7.7, 1 mM EDTA, 0.1 mM Neocuproine) with 1% Triton X100, protease, and phosphatase inhibitors and cleared by centrifugation at 16,000 g at 4 °C for 10 min. Protein was quantified by Bradford assay and samples were normalized for protein content. Sample free thiols were blocked in methyl methanethiosulfonate (MMTS) at 50 °C for 20 min with shaking. Protein in samples was precipitated with cold acetone and washed twice with at RT with 70% acetone. Protein pellets were resuspended in HENS (HEN buffer with 1% SDS) buffer and biotin-HPDP for biotinylation of sulfhydrated cysteines. Samples were incubated for 75 min at RT with rotation. Proteins were precipitated twice with cold acetone followed by resuspension in HENS buffer. Neutralization buffer (20 mM HEPES-NaOH, pH 7.7, 100 mM NaCl, 1 mM EDTA, 0.5% Triton X-100) was added, and inputs were reserved for loading on SDS-PAGE. Neutravidin agarose beads were added to the samples and incubated at 4 °C overnight with rotation. Beads were washed with neutralization buffer with high salt (Neutralization buffer with 600 mM NaCl) seven times followed by addition of elution buffer (20 mM HEPES-NaOH, pH 7.7, 100 mM NaCl, 1 mM EDTA, 1% β-mercaptoethanol) and incubation at 95 °C for 5 min. LDS buffer with DTT was added and samples were loaded on SDS-PAGE and immunoblotted with indicated antibodies. The dimedone switch assay was conducted essentially as described earlier (6).

Mass Spectrometry for Identification of Sulfhydrated Cysteines

Purified GST-GSK3β was incubated with 100 uM NaSH in HEN buffer (HEPES–NaOH, pH 7.7, 250 mM EDTA, 1 mM Neocuproine 0.1 mM) for 1 h at 37 °C followed by FASP digest on a 30 kDa filter by trypsin overnight at 37 °C. Filter was washed, acidified, and peptides were eluted with 60% ACN/.1% TFA and were run immediately on high-resolution mass spectrometry for analysis. MS-MS spectra was searched using PEAKSX against the database created from MASCOT. Fragment Mass Error Tolerance was 0.012 Da and Parent Mass Error Tolerance was 6 ppm. MASCOT was set to search NP_002084.2 (glycogen synthase kinase-3 beta isoform 1 [*Homo sapiens*]). Human recombinant Tau 441 was incubated with H_2O_2 and H_2S mixture to induce protein persulfidation and labeled with dimedone switch method as described earlier (39). Untreated samples served as a control. Proteins were subjected to trypsin digestion and LC/MS/MS analysis. Obtained spectra were analyzed with PEAKSX. The search settings were: precursor Δm tolerance = 10 ppm, fragment Δm tolerance = 0.2 Da, missed cleavages = 2, -10logP>50, modifications of lysine: NBF (163.0012), modifications of cysteine: NBF (163.0012), dimedone (138.0681),

Purified Recombinant proteins

WT Tau and Tau C291S/C322S were purified from BL21 bacterial cells transformed with pTrcHis-Tau or pTrcHis-Tau C291S/C322S, respectively. Site-directed mutagenesis was carried out to generate the Tau mutant plasmid. Capturem His-Tagged Purification Maxiprep Columns (Takara) were used to purify the recombinant Tau proteins and visualized by SDS gel electrophoresis on 4-12% Bis-Tris polyacrylamide gels, followed by Coomassie staining using SimplyBlue SafeStain (Thermo Fisher Scientific). GST-CSE was purified by affinity chromatography using glutathione-agarose (Sigma) as per the manufacturer's recommendations.

Tau phosphorylation assays

HEK293 cells were transfected with indicated plasmids for 24 h. Cells were treated with 100 μM NaSH for 24 h and then lysed in IP buffer with clearance of lysates by centrifugation at 16,000 g for 10 min. Protein was quantified by Bradford assay and samples were normalized for protein content. LDS buffer with DTT was added and samples incubated at 95 °C for 5 min. Samples were loaded on SDS-PAGE and immunoblotted with indicated antibodies. For the *in vitro* assays, the kinase activity assay provided with the SignalChem GSK3β purified protein. Either 10 μL of GSK3β (0.02 μg/uL) diluted in kinase dilution buffer III (KDBIII), containing 5 mM MOPS, pH 7.2, 2.5 mM β-glycerophosphate, 5 mM $MgCl_2$, 1 mM EGTA, 0.4 mM EDTA and 50 ng/μL BSA or 10 μL of KDBIII, 5 μL of 15 μM purified Tau, and 5 μL of dH_2O or 0.5 mM NaSH in dH_2O (stock solution). Subsequently 5 μL of 0.25 mM ATP was added to each reaction and incubated in the shaking incubator for 15 min at 30 °C. Next, LDS (+DTT) was added to stop the reactions and incubated at 95 °C heat block for 5 min followed by Western blot analysis.

Radioactive assay for determination of GSK3β activity: For the radioactive *in vitro* assays, the kinase activity assay using GSK3β purified protein (SignalChem) was utilized. Either 10 μL of GSK3β (0.02 μg/uL) diluted in kinase dilution buffer III (KDBIII), containing 5 mM MOPS, pH 7.2, 2.5 mM β-glycerophosphate, 5 mM $MgCl_2$, 1 mM EGTA, 0.4 mM EDTA and 50 ng/μL BSA or 10 μL of KDBIII, 5 μL of 15 μM purified Tau, and 5 μL of dH_2O or 0.5 mM NaSH in dH_2O (stock solution). Subsequently 5 μL of 0.25 mM [γ-^{32}P] ATP (1 mCi/100 μl) was added to each reaction and incubated in the shaking incubator for 15 min at 30 °C. Next, the reaction mixture was spotted onto individually precut strips of phosphocellulose P81 paper, which were air dried and washed with 1% phosphoric acid in double distilled water and subjected to scintillation counting to estimate the radioactivity incorporated into the peptide.

Mouse behavioral studies

Barnes maze test: 6-mo old WT and 3xTg-AD mice were treated with daily intraperitoneal injections of NaGYY (100 mg/kg) or saline (vehicle) as indicated for 12 wk until behavioral assays were performed as indicated at 9-mo. Mice were trained on the Barnes Maze platform twice a day for four days followed by testing on the fifth and twelfth days. Training and testing were carried out as follows: mice were placed in the middle of a raised platform with visual cues in the periphery and 20 holes along the edge, one of which contained an escape path for the mouse. For a maximum of three min, the number of nose pokes into correct and incorrect holes as well as the time until the mouse nose poked the correct hole and the time until the mouse entered the escape path were recorded. If a mouse entered the escape path prior to the three-min limit, the session was cut short.

Open field test. The mouse cohort used for the Barnes maze test was run on an open field chamber with IR beams recording their locomotor activity. Mice were allowed to freely roam the chamber for 45 min.

Antibody array assessment of GSK3β sulfhydration. Antibody-array like detection of GSK3β sulfhydration from human brain samples. The GSK3β antibody (sc-377213, Santa Cruz) was immobilized on a 96 well plate with NHS-activated surface as described previously (6). Considering that proteins are labelled with NBF (green) for total load and with Cy5 (red) for sulfhydration, measuring the ratio of the two signals yields the levels of GSK3b sulfhydration. As a negative control 488-labelled albumin (instead of antibody) was used to block the available surface and then incubated with control lysates.

Statistical Analysis. Results are presented as means ± SEM for at least three independent experiments. The sample sizes used were based on the magnitude of changes and consistency expected. Statistical significance was reported as appropriate. *P* values were calculated with Student's *t* test. In behavioral analyses, the experimenter conducting the test was blinded to the genotype or treatment of the animals under study. Statistical significance was calculated using one-way ANOVA/post-hoc Tukey test.

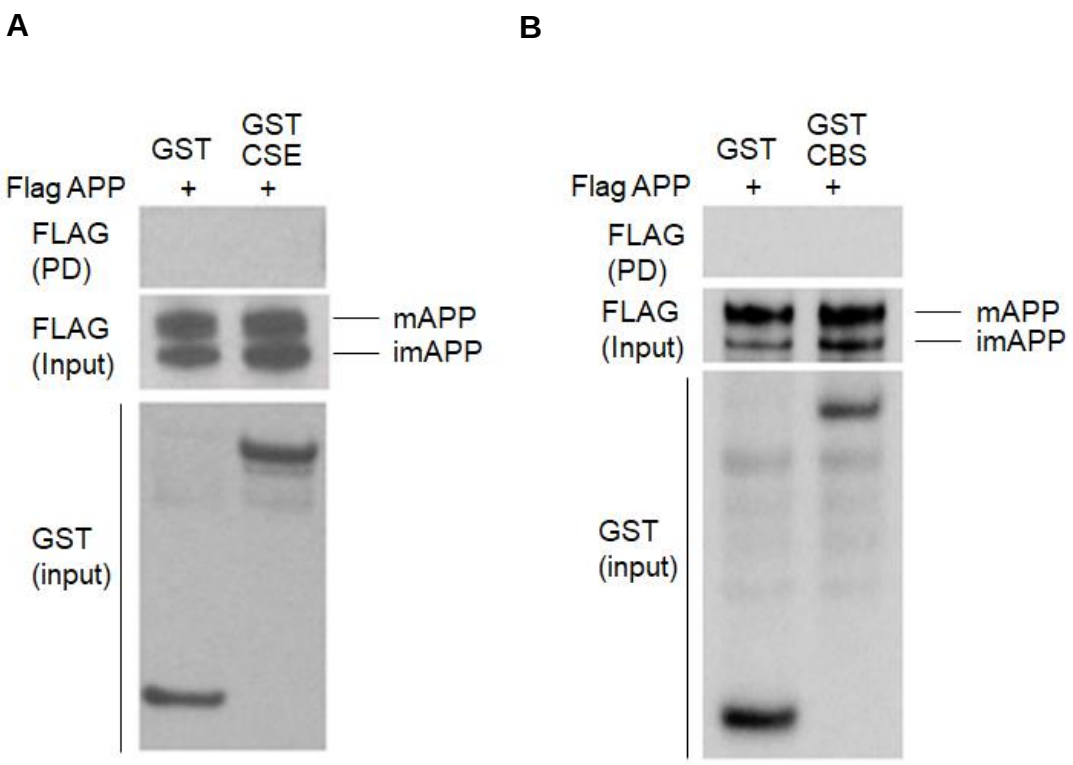

Fig. S1. Amyloid precursor protein (APP) does not interact with cystathionine γ-lyase (CSE) and cystathionine β-synthase (CBS). (*A*) CSE does not bind APP. HEK293 cells were transfected with FLAG APP and either GST alone or GST-CSE for 24 h and GST pulldown conducted using glutathione agarose. Western blot analysis was performed after the pull-down, APP exists in cells as two forms, the immature form (imAPP), which is *N*-glycosylated and *O*-glycosylated. CSE does not bind to APP as seen in the pull-down (PD) using anti-FLAG antibodies. (*B*) CBS does not bind APP. HEK293 cells were transfected and processed as described above and analyzed by Western blot analysis.

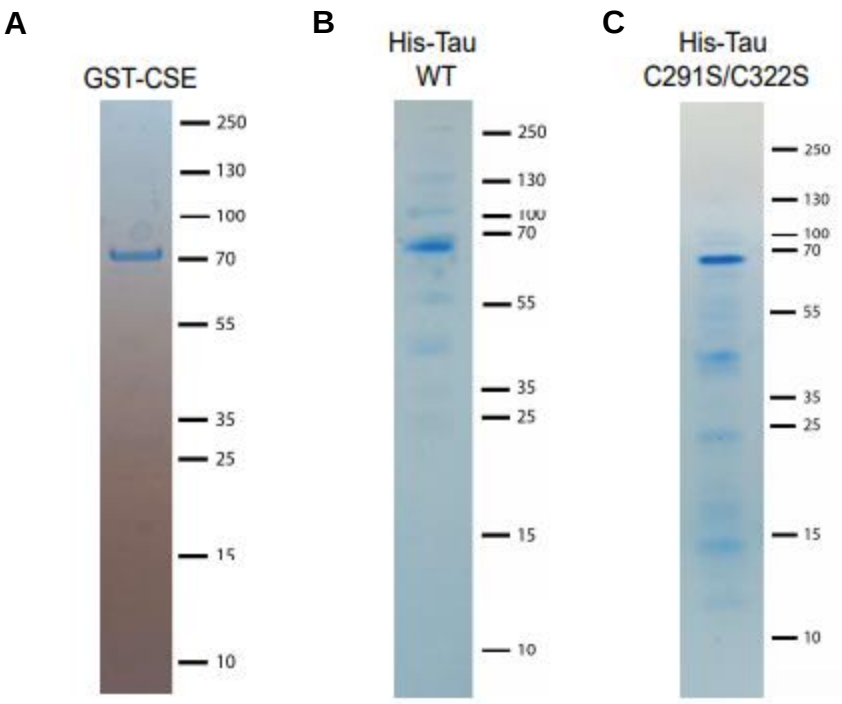

Fig. S2. Protein purification profiles of Tau, its mutants and cystathionine γ-lyase (CSE). (*A*) GST- tagged CSE was purified using glutathione agarose and analyzed by Coomassie staining. (*B,C*) His-tagged wild type Tau and the double cysteine mutant, Tau C291S/C322S was purified using CaptureEm purification systems (Takara) and purity confirmed by SDS gel electrophoresis and Coomassie staing as described earlier.

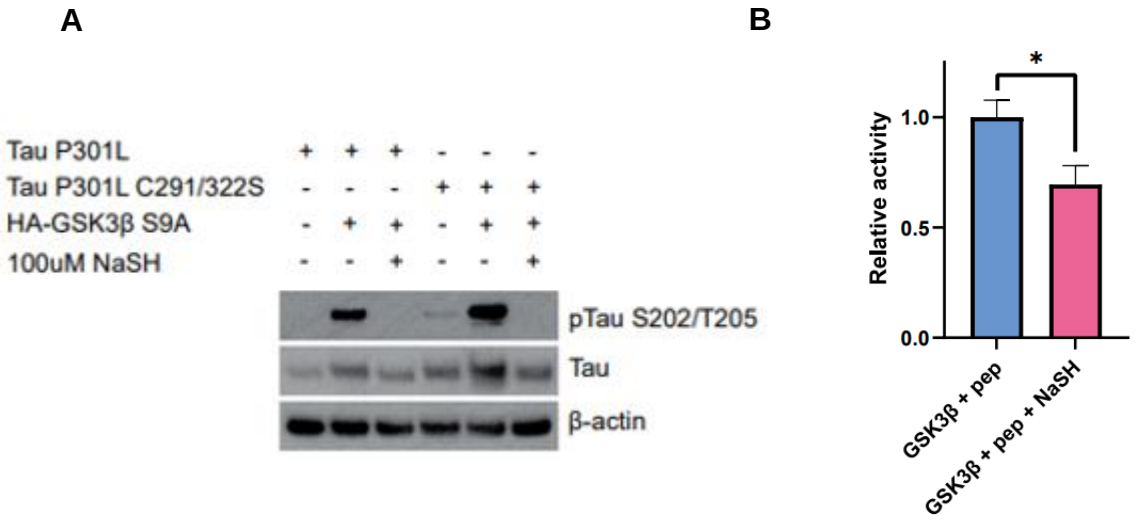

Fig. S3. Glycogen synthase kinase 3β (GSK3β) activity assays. (*A*) H_2S inhibits phosphorylation of Tau P301L by GSK3β. HEK293 cells were transfected with Tau P301L or Tau P301LCys291/Cys322 and GSK3β and treated with 100 μM NaSH for 24 h and analyzed for phosphorylation of Tau at Ser202 and Thr205 by western blotting. While GSK3β phosphorylated Tau, NaSH prevented this phosphorylation. (*B*) The H_2S donor, NaSH prevents phosphorylation of a peptide substrate of Tau by GSK3β (YRRAAVPPSPSLSRHSSPHQ**pS**EDEE, derived from glycogen synthase). Active GSK3β, peptide substrate and [γ-^{32}P] -ATP were incubated at 30 °C for 15 min, followed by (n=6, SEM, **P* <0.05).

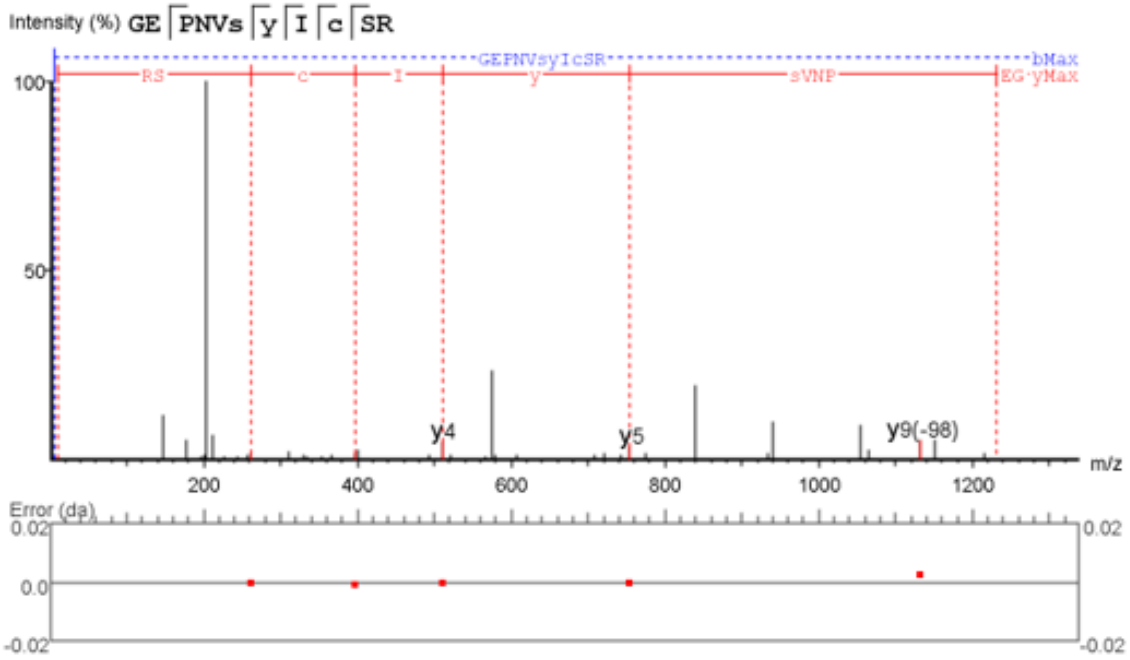

Fig. S4. LC-MS/MS spectra for identification of sulfhydration of GSK3β at Cysteine 218.

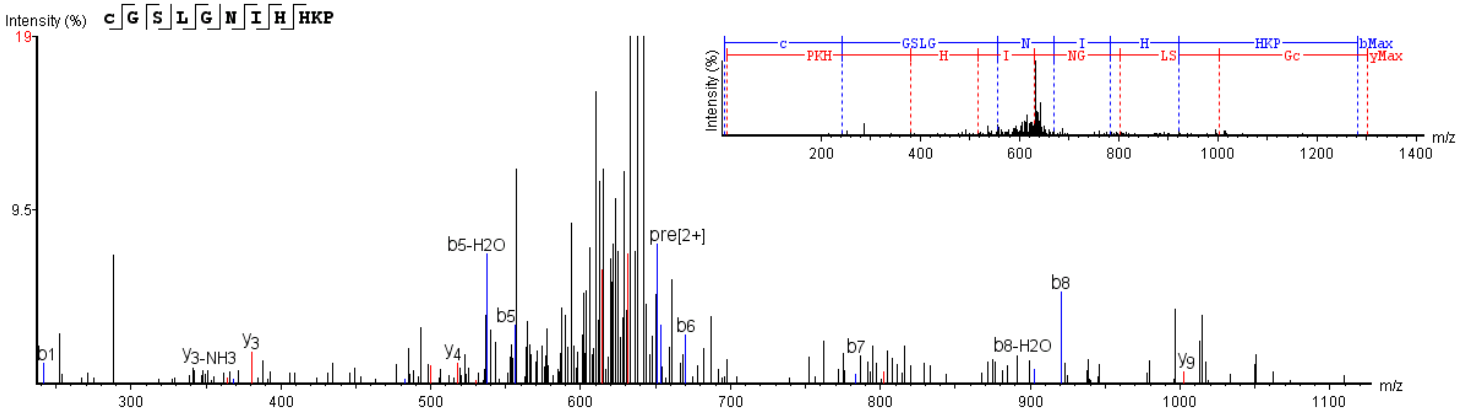

Fig. S5. MS/MS spectra of sulfhydrated C322 containing peptide of Tau labelled with dimedone, using dimedone switch method.

SI References

1. M. Whiteman *et al.*, Phosphinodithioate and Phosphoramidodithioate Hydrogen Sulfide Donors. *Handb Exp Pharmacol* **230**, 337-363 (2015).
2. B. E. Alexander *et al.*, Investigating the generation of hydrogen sulfide from the phosphonamidodithioate slow-release donor GYY4137. *MedChemComm* **6**, 1649-1655 (2015).
3. E. Latorre, R. Torregrossa, M. E. Wood, M. Whiteman, L. W. Harries, Mitochondria-targeted hydrogen sulfide attenuates endothelial senescence by selective induction of splicing factors HNRNPD and SRSF2. *Aging (Albany NY)* **10**, 1666-1681 (2018).
4. T. Chiku *et al.*, H_2S biogenesis by human cystathionine gamma-lyase leads to the novel sulfur metabolites lanthionine and homolanthionine and is responsive to the grade of hyperhomocysteinemia. *J Biol Chem* **284**, 11601-11612 (2009).

5. A. K. Mustafa *et al.*, H_2S signals through protein S-sulfhydration. *Sci Signal* **2**, ra72 (2009).
6. J. Zivanovic *et al.*, Selective Persulfide Detection Reveals Evolutionarily Conserved Antiaging Effects of S-Sulfhydration. *Cell Metab* **30**, 1152-1170 e1113 (2019).
7. M. S. Vandiver *et al.*, Sulfhydration mediates neuroprotective actions of parkin. *Nat Commun* **4**, 1626 (2013).